Insulating surface layer on single crystal K3C60

Schiessling, J.; Kjeldgaard, L.; Kaambre, T.; Marenne, I.; Qian, L.; O'Shea, J.N.; Schnadt, J.; Garnier, M.G.; Nordlund, D.; Nagasono, M.

Published in:
European Physical Journal B

DOI:
10.1140/epjb/e2004-00335-2

Publication date:
2004

Eur. Phys. J. B **41**, 435–438 (2004)
DOI: 10.1140/epjb/e2004-00335-2

THE EUROPEAN PHYSICAL JOURNAL B

Insulating surface layer on single crystal K_3C_{60}

J. Schiessling[1,4,a], L. Kjeldgaard[1], T. Käämbre[1], I. Marenne[2], L. Qian[1], J.N. O'Shea[1], J. Schnadt[1], M.G. Garnier[3], D. Nordlund[3], M. Nagasono[3], C.J. Glover[3], J.-E. Rubensson[1], N. Mårtensson[1,3], P. Rudolf[2,4], J. Nordgren[1], and P.A. Brühwiler[1,5,b]

[1] Department of Physics, Uppsala University, Box 530, 751 21 Uppsala, Sweden
[2] LISE, Facultés Universitaires Notre Dame de la Paix, Rue de Bruxelles 61, 5000 Namur, Belgium
[3] MAX-lab, University of Lund, Box 118, 22100 Lund, Sweden
[4] Materials Science Centre, University of Groningen, Nijenborgh 4, 9747 AG Groningen, the Netherlands
[5] EMPA, Lerchenfeldstrasse 5, 9014 St. Gallen, Switzerland

Received 16 July 2004
Published online 5 November 2004 –

Abstract. Using angle-dependent photoemission spectra of core and valence levels we show that metallic, single crystal K_3C_{60} is terminated by an insulating or weakly-conducting surface layer. We attribute this to the effects of strong intermolecular correlations combined with the average surface charge state. Several controversies on the electronic structure are thereby resolved.

PACS. 71.20.Tx Fullerenes and related materials; intercalation compounds – 73.20.-r Electron states at surfaces and interfaces – 79.60.Bm Clean metal, semiconductor, and insulator surfaces

Rapid Note

Studies on the A_3C_{60} family continue to expose important aspects of superconductivity in correlated materials [1–6], after a largely successful explanation of the superconductivity in terms of standard Bardeen-Cooper-Schriefer (BCS) theory [7,8]. K_3C_{60} with a T_C of 19 K has become the primary testing ground of fulleride superconductivity. One of the key quantities in any theory of superconductivity or metallicity is the finite density-of-states at the Fermi level, $N(E_F)$ [3,4,8]. The distribution of the density-of-states is another, whose structure-dependence, e.g., has implications for superconductivity [3,8]. Both of these aspects of the electronic structure are in principle accessible experimentally in photoelectron spectroscopy (PES), which was indeed instrumental in the initial identification of the alkali fulleride phases [9,10], and was used, e.g., to characterize the BCS-like gap in K_3C_{60} and Rb_3C_{60} [11]. However, there are discrepancies between the theoretical description and experimental observations in the magnitude of important quantities. E.g., the LUMO-derived conduction band as observed in PES is much broader than theory predicts, suggesting that PES-derived determinations of $N(E_F)$ are unreliable [8], with the result that the character of the surface electronic structure of single crystal K_3C_{60} has been strongly debated. The discussion was based on virtually identical spectra: in one model, the surface fulleride layer has a charge of -3 per molecule as in the bulk, and with an identical electronic structure [10,12–17]; in the other model, the average charge is -1.5 or -2.5, with a primary role for the surface implied for superconductivity [11,18]. While the latter view is somewhat controversial, it is the only work thus far which incorporates the important effects of ionicity on the allowed surface structures [18]. In both models, many-body effects are deduced to play a dominant role in the experimentally observed density-of-states [6,8,11,14,16–18], placing constraints on their theoretical description.

These constraints turn out to be greatly relaxed (towards the current theoretical picture [1,8]) if one admits the possibility of an insulator-like surface electronic structure. This has been ruled out previously based on a fundamental assumption that the spectra contain no observable subsurface contributions [11,12,16,17]. We show for the first time using angle-dependent PES that the subsurface contributions can be clearly identified, and are derived from a metallic state. This implies that the PES measurement of a BCS-like gap opening at E_F is associated with a direct measurement on the bulk superconductor, and not a proximity effect or exotic surface metallic state [11,18]. The surface contribution is also extracted, characterized as due to an insulating phase, and shown for all bands except the LUMO-derived conduction band to dominate the spectra. We rationalize the occurence of this phase in terms of a half-integer charge state [18] at the surface of the ionic compound K_3C_{60}, whose overall insulating character is driven by intermolecular electronic correlation effects.

The experiments were carried out at Beamline I511 at MAX-lab [19] at MAX-lab, Sweden, which is comprised of a modified SX700 monochromator and a Scienta 200 photoelectron analyzer. The spectra were excited using linearly-polarized undulator light incident

[a] e-mail: joachim.schiessling@fysik.uu.se
[b] e-mail: paul.bruehwiler@empa.ch

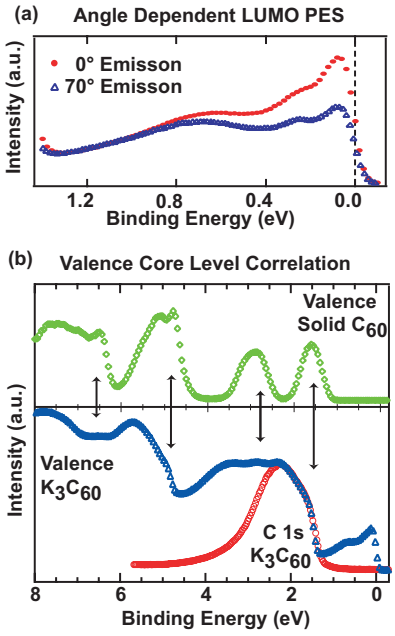

Fig. 1. (a) Photoelectron spectra of the LUMO-derived band at the indicated emission angles. (b) Comparison of solid C_{60} to K_3C_{60} valence spectra taken at normal emission, showing the one-to-one correlation between each band in the former with a small feature marking the beginning of a band in the latter. The red curve is a C 1*s* spectrum, also at normal emission, shifted to show the excellent correlation with HOMO-derived features of the valence band.

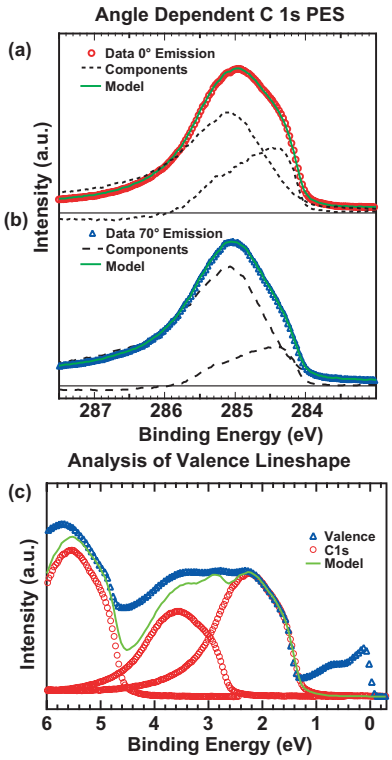

Fig. 2. (a) and (b): C 1*s* spectra at the indicated emission angles. The low energy shoulder is marked with a vertical line. Also shown are the difference spectra obtained as described in the text, isolating the bulk and surface components. (c) Approximation of the valence spectrum obtained by placing a C 1*s* spectrum at each point indicated in Figure 1b, showing that the spectrum can be interpreted as a composite similar to the C 1*s*.

at about 82° from normal; note that the direction of radiation incidence was (almost) in the plane of the sample surface and sample and analyzer could be rotated around the direction of light incidence.

The K_3C_{60} single crystal sample was prepared in situ in a standard UHV preparation chamber with a base pressure of 2×10^{-10} by the so-called vacuum distillation procedure [20]. Alternating layers of C_{60} and K were sublimated onto the (111) surface of a clean Cu crystal. After each deposition cycle the stoichiometry was checked with PES to be below $x = 3$ in this stage of sample preparation, using published spectra [14,20] as references. After the deposition was completed the sample was annealed at 600 K for 6 hours to sublime excess C_{60}, resulting in a single phase. The typical hexagonal low energy electron diffraction pattern was obtained. The photon energy (energy resolution, analyzer acceptance angle) was 110 eV for the LUMO (40 meV, 4°), valence spectra (80 meV, 6°) and 350 eV (150 meV, 9°) for the C 1*s*. The large photoelectron analyzer acceptance angle ensured that information from the entire Brillouin Zone was collected. The polarization was aligned along the emission direction to maximize the excitation cross section [21,22].

The LUMO-derived spectra of a single crystal of K_3C_{60} are shown in Figure 1a, taken at two emission angles. The spectra strongly resemble previous spectra of single crystal [11,12,14,18] and other high-quality samples [10,16]. It is apparent that the ratio of the spectral intensity near E_F to that at 0.6–0.8 eV decreases as the emission angle increases. We will show that this is because the intensity near E_F is associated with bulk states, in accord with the short mean free path for electrons at this energy [22].

The clearest evidence for the presence of different phases in the sample is seen in the spectra of the deeper levels, as shown in Figure 1b. These have a complex structure, much richer than that of pure C_{60}, in spite of the theoretical expectation of quite comparable separation and width for both cases [23]. We note first the excellent correlation between the C_{60} and K_3C_{60} spectra: the HOMO-derived and deeper bands show an almost one-to-one correspondence, here visualized by associating a shoulder or small intermediate peak in K_3C_{60} with each of the C_{60} bands. Moreover, for each such structure, there is a second, stronger peak to higher binding energy throughout the K_3C_{60} spectrum. The K_3C_{60} C 1*s* spectrum, placed for comparison below the valence data, gives a second example of such a structure, which closely matches the intensity distribution of the onset of the HOMO-derived intensity. The binding energy difference between C 1*s* and HOMO is virtually constant for all cases of charge transfer to C_{60} [22], especially for the ordered bulk fullerides at different alkali concentrations, including pristine solid C_{60}. Hence the excellent agreement in the lineshape is not surprising if the doublet structure can be traced to fulleride ions at different charge states near the surface of the sample.

We next analyze the relatively simple C 1*s* line in terms of its components, to subsequently elucidate the valence manifold. This analysis is visually summarized in Figures 2a and b. Spectra taken at different emission angles are seen to have different component intensity ratios, comparing the shoulder at low binding energy to the main peak. By taking such spectra and scaling one to match the other at high or low binding energy, difference spectra are obtained which resolve the data into two components: a weaker one at low binding energy with an asymmetric profile, and a stronger, almost symmetric line at higher binding energy [24]. Only one of the phases represented by these peaks can correspond to the bulk. The

Rapid Note

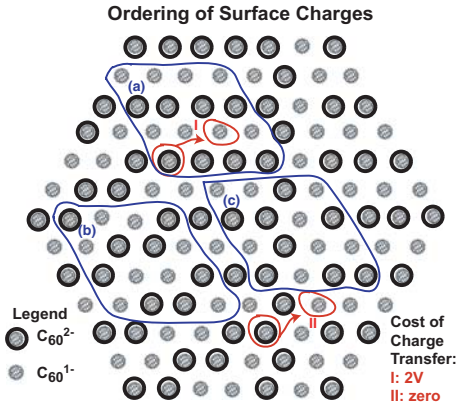

Fig. 3. Possible charge arrangements of the K_3C_{60} (111) surface consistent with the present results and the considerations of reference [18]. Three fundamental kinds of domain can exist given the average charge of –1.5 on each surface fulleride ion: (a) line CDW, (b) zig-zag CDW or (c) "random". The charge state of (doubly-) singly-charged molecules is indicated by (large) small circles. The transitions indicated are discussed in the text.

angle dependence of the intensity suggests that this is the lower-binding-energy component [25], qualitatively similar to the variation at E_F in Figure 1a. Hence the lineshape and position at lower binding energy suggest that the bulk is metallic. The larger intensity, symmetric lineshape, and higher binding energy suggest preliminarily that the second component is due to an insulating surface layer, a point which we develop further below.

Figure 2c shows that the valence data can be modelled reasonably well by taking the C 1*s* line as an empirical model for the doublet pattern already identified, guided by the pure C_{60} valence spectrum as in Figure 1b, thus further supporting the hypothesis that the spectrum is a composite of at least two subspectra. Notably, the minor peak at about 2.9 eV in K_3C_{60} is reproduced automatically, as are the overall intensity relationships.

How would such an insulating surface phase arise? A key point was raised in reference [18], that the surface termination can only take one of several allowed configurations, to avoid setting up unphysically-large electric fields in the sample. Those authors proposed an average charge per fulleride at the surface of –1.5 or –2.5 as likely possibilities; based on the fact that K_3C_{60} films are quite nonreactive in UHV, we make the ansatz that –1.5 is correct, since only this termination places all K ions below a surface C_{60} layer. An average fulleride charge of –1.5 corresponds to equal populations of fulleride ions at –1 and –2 in the surface layer. All sites are equivalent due to the symmetry of the K and C_{60} layers below, so that these charges can fluctuate [22]. Figure 3 illustrates allowed, highly-ordered distributions, which would be either one of two kinds of charge density waves.

Due to the fact that the surface layer is not a bipartite lattice, the charge distribution can adopt much less ordered structures without energy cost. Considering the transport properties of such a layer, note that an electron hopping from a doubly- to singly-charged molecular site does not incur the net cost U, the on-site correlation energy incurred for transfer between sites of like charge [8]. Instead, the nearest-neighbor correlation, V, dominates [26]. Transition I is the lowest energy transfer of an electron in an ordered domain, (A) or (B), which removes the electron from all possibility of interacting with the starting site, thus corresponding to a fundamental excitation over the (correlation-induced) gap at the surface. The transfer to a nearest-neighbor singly-charged site involves a net barrier of V, i.e., the energy of a charge transfer exciton in such a domain, whereas a transfer like I shown in Figure 3 would require excitation by 2 V, corresponding to the minimum transport gap. In a lower-symmetry configuration, transitions such as II are enabled, in this case without energy cost, making such configurations in principle metallic [18]. However, the latter transitions will have a low probability, because of the weak transfer integral corresponding to a minimum pathlength of two fullerene spacings, suggesting that the surface could retain much of the insulator aspects of the ordered domains even in this case. Furthermore, there is very little intensity at E_F from the larger peak obtained in the analysis of Figure 2a, suggesting empirically that metallic configurations in the surface layer are sparse.

This model of the electronic structure has measurable consequences in PES. We take the single-particle energy difference between singly- and doubly-occupied LUMO orbitals to be negligible, and note that the energies of photoelectrons extracted from these two kinds of sites incorporate terms in U and V, given by the difference in the initial and final state configurations [22]. In an ordered domain, these terms give $U + 8V$ for a doubly-occupied site, and $10V$ for a singly-occupied site, for a difference of $U - 2V$, with the doubly-occupied site at higher energy. Taking the values of U (1.1 eV) and V (0.35 eV) for negatively-charged molecules [26], this yields a separation of 0.4 eV. This result will remain valid in the simplest approximation for PES out of all orbitals on a molecule, since a hole in a deeper level will neutralize one charge in the LUMO when considering the correlation energies, much as the hole-hole interaction is only weakly dependent on the choice of orbital [27]. Hence the ordered surface should yield two almost identical spectra split by approximately 0.4 eV, with broadening of the spectra to the extent that electronic disorder exists (config. case (c) of Fig. 3). This provides a natural explanation for the broad surface component found in the C 1*s* and deeper valence bands, suggesting that each itself is a doublet, with sub-peaks of equal intensity.

The LUMO-derived conduction band remains to be understood, although we expect three components just as for the other bands. Because the LUMO is partially occupied, the intensity of each component will be scaled according to the instantaneous local electron population. Thus, the bulk layers whose spectrum starts at E_F are scaled by a factor of 3, the doubly-charged sites located somewhat below E_F are scaled by a factor of 2, and the singly-charged sites located about 0.4 eV further from E_F by a factor of 1. To model these effects, we take the line

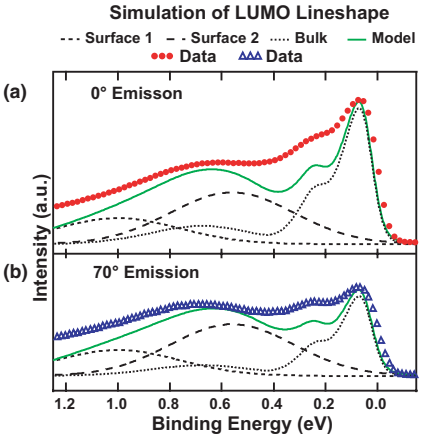

Fig. 4. Simulation of the LUMO-derived lineshape based on the analysis in Figure 2, and the energetics of PES implied by Figure 3, as described in the text.

profile of reference [28] as a first order approximation of the lineshape for bulk K_3C_{60} [6], and model the plasmon coupling according to reference [16]. We use the C 1*s* analysis to give the overall surface to bulk intensity ratio, and to place the surface components, noting that they should be symmetrically arranged about the center of the total surface contribution, which in turn lies at about E_F −0.8 eV. Starting from the intensity ratio found there at each of the two emission angles, we apply the scaling factors, and include these additional two lines, as shown in Figure 4. We see that the model spectra produced in this manner reflect all major features of the experiment, including the angle dependence of Figure 1a. This lends strong support to the relatively simple model of the spectrum suggested earlier [16].

The present results provide natural explanations for the broad features in the deeper bands of K_3C_{60}, and the uniquely different lineshape of the LUMO band in comparison; this result is strongly supported by a bulk measurement of the density-of-states using X-ray emisson [29]. Other open questions can also be resolved. For instance, the common temperature – [14] and [18] doping-dependence of the intensity of the Fermi edge and the first shoulder of the HOMO-derived band follow from the fact that they are both features of triply-charged bulk molecules. More importantly, there is no need to invoke the proximity-effect to explain the opening of a BCS-like gap in the PES spectrum [11], since the states near E_F reflect the bulk.

These results thereby resolve long-standing as well as recent conflicts between the theoretical consensus and experimental pictures of the alkali fulleride high temperature superconducting compounds. The present model of the LUMO-derived conduction band in the bulk is seen to describe the density-of-states near E_F semiquantitatively, and is quite similar to that directly observed for a K-doped monolayer [6], suggesting that the differences between these systems are subtler than previously suspected. It remains to be seen if the band dispersion of the bulk states can be measured at a level comparable to a monolayer [6], but would provide a more direct view of the fulleride superconductor electronic states, directly probing the effects of the stronger correlations expected [30] and three-dimensional character.

We would like to thank W. Eberhardt for making the C_{60}^- data available to us. I. Marenne acknowledges for financial support the FRIA, Belgium. This work was performed within the EU-TMR "FULPROP" network, contract no ERBFMRX-CT97-0155, with additional funding from the EU Access to Large Scale Facilities Program. We acknowledge our founding sources, the Belgian National Fund for Scientific Research (FNRS), Netherlands Foundation for Fundamental Research on Matter (FOM), Vetenskapsrådet and Göran Gustafsons Stiftelse as well as the Consortium on Clusters and Ultrafine Particles, which in turn is supported by Stiftelsen för Strategisk Forskning.

References

1. J.E. Han, O. Gunnarsson, V.H. Crespi, Phys. Rev. Lett. **90**, 167006 (2003)
2. P. Durand et al., Nature Materials **2**, 610 (2003)
3. Y. Iwasa, T. Takenobu, J. Phys.: Condens. Matter **15**, R495 (2003)
4. M. Capone, M. Fabrizio, C. Castellani, E. Tosatti, Science **296**, 2364 (2002)
5. R. Yamachika, M. Grobis, A. Wachowiak, M.F. Crommie, Science **304**, 281 (2004)
6. W.L. Yang et al., Science **300**, 303 (2003)
7. C.M. Varma, J. Zaanen, K. Raghavachari, Science **254**, 989 (1991)
8. O. Gunnarsson, Rev. Mod. Phys. **69**, 575 (1997)
9. P.J. Benning et al., Science **252**, 1417 (1991)
10. C.T. Chen et al., Nature **352**, 603 (1991)
11. R. Hesper, L.H. Tjeng, A. Heeres, G.A. Sawatzky, Phys. Rev. Lett. **85**, 1970 (2000)
12. A. Goldoni, S.L. Friedmann, Z.-X. Shen, F. Parmigiani, Phys. Rev. B **58**, 11023 (1998)
13. A. Goldoni et al., Phys. Rev. B **59**, 16071 (1999)
14. A. Goldoni et al., J. Chem. Phys. **113**, 8266 (2000)
15. A. Goldoni et al., Phys. Rev. Lett. **87**, 076401 (2001)
16. M. Knupfer et al., Phys. Rev. B **47**, 13944 (1993)
17. P.A. Brühwiler et al., Phys. Rev. B **48**, 18296 (1993)
18. R. Hesper, L.H. Tjeng, A. Heeres, G.A. Sawatzky, Phys. Rev. B **62**, 16046 (2000)
19. R. Denecke et al., J. Electron. Spectrosc. Relat. Phenom. **103**, 971 (1999)
20. D.M. Poirier, Appl. Phys. Lett. **64**, 1356 (1994)
21. J. Schiessling et al., Phys. Rev. B **68**, 205405 (2003)
22. J. Schiessling et al. (unpublished)
23. S. Satpathy et al., Phys. Rev. B **46**, 1773 (1992)
24. The line shapes determined this way are not ideal, with, e.g., an excursion to negative intensity for the weaker component. This is primarily due to the increase in inelastic scattering at higher emission angles, which shifts a fraction of the intensity from low to high binding energy
25. We note that a more complex explanation in terms of photoelectron diffraction is highly unlikely: Angle-dependent PES of C_{60} multilayers does not show diffraction-induced fine structures for electrons with kinetic energies near 100 eV [21]
26. V.P. Antropov, O. Gunnarsson, O. Jepsen, Phys. Rev. B **46**, 13647 (1992)
27. R.W. Lof, M.A. van Veenendaal, H.T. Jonkman, G.A. Sawatzky, J. Electron Spectrosc. Relat. Phenom. **72**, 83 (1995)
28. O. Gunnarsson et al., Phys. Rev. Lett. **74**, 1875 (1995)
29. T. Käämbre et al. (unpublished)
30. R. Hesper, L.H. Tjeng, G.A. Sawatzky, Europhys. Lett. **40**, 177 (1997)

Rapid Note